Method for thermal diffusivity measurements based on photothermal deflection

M. Bertolotti, G. Liakhou,[a] R. Li Voti, F. Michelotti, and C. Sibilia
Dipartimento di Energetica, Universita' di Roma "La Sapienza" Via Scarpa 16, 00161 Roma, Itlay

(Received 5 November 1992; accepted for publication 30 August 1993)

The thermal diffusivity measurement through pulsed photodeflection in a modified collinear configuration is presented and discussed; comparison between theory and experiment is also shown.

I. INTRODUCTION

The photothermal deflection method in its collinear configuration with a pulsed pump beam has been used to measure low absorption ($\approx 10^{-6}$ cm^{-1}) coefficients.[1-3] For the determination of thermal diffusivity, the technique is used with a periodically modulated pump beam.[4] Alternatively a pulsed "flash" method is currently used;[5,6] however this method is not useful for thin samples.

In the present article it is shown how the photothermal deflection in collinear configuration can be used with a pulsed beam to measure the thermal diffusivity by studying the time evolution of the deflection signal in a very simple way which also allows one to determine the thermal spot size dimension. In this method the time $t_{\max}$ at which the deflection of a probe beam, traveling at some suitable distance from the pump beam, reaches its maximum value is measured.

After some theoretical considerations and numerical simulations, the method is applied to the experimental measurement of thermal diffusivity of a glass sample giving results in excellent agreement with previously known values.

II. THEORY

The problem of the determination of the temporal behavior of the photodeflection signal in collinear configuration for a pulsed pump has been discussed for some time.[1,2]

In this configuration (Fig. 1), the expression for the deflection angle along the radius r is given by

$$\Phi(r,t)=\frac{1}{n}\frac{\partial n}{\partial T}\int_{\text{path}}\frac{\partial}{\partial r}T(r,t)dz, \tag{1}$$

where n is the refractive index, $\partial/\partial r$ is the derivative along the direction perpendicular to the ray path z, and $T(r,t)$ is the temperature increasing. The determination of the thermal field is obtained solving the Fourier equation for the ith medium,

$$\nabla^2 T_i(r,t)-\frac{1}{D_i}\frac{\partial T_i(r,t)}{\partial t}=-\frac{W_i(r,t)}{k_i}, \tag{2}$$

where D_i, k_i, and $W_i(r,t)$, respectively, are the thermal diffusivity, thermal conductivity, and the power density transformed into heat in each ith medium. Because the air is transparent, the only source term is W_1, which for a pulse of duration t_0 can be written

$$W_1(r,t)=\frac{2\tau\alpha E}{\pi a^2}\exp\left[-2\left(\frac{r}{a}\right)^2-\alpha z\right]f_{t_0}(t), \tag{3}$$

where a is the pump spot-size, $\tau=(1-R)$, R is the reflection coefficient at the interface between air and the sample, α is the absorption coefficient of the sample, E is the pulse energy, and $f_{t_0}(t)$ is the temporal form factor of the pulse which is defined such that

$$\int_0^\infty f_{t_0}(t)dt=1.$$

Using Laplace transforms to solve Eq. (2) for a slab of length L, we obtain

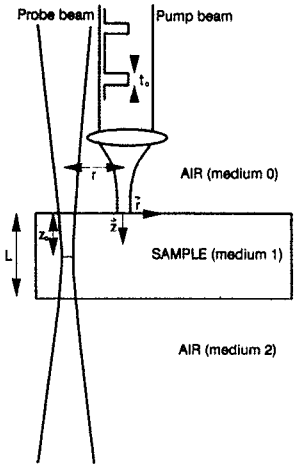

FIG. 1. Schematic representation of the configuration.

[a]On leave from: Technical University of Moldova, Stefan Cel Mare 168, 277012 Kishinev, Moldova.

 0021-8979/93/74(12)/7078/7/$6.00

$$T(r,z,s)=F(s)\frac{\tau\alpha E}{2\pi k_1}\int_0^\infty \frac{\delta J_0(\delta r)\exp[-(\delta a)^2/8]}{\beta_1^2-\alpha^2}\times\left(\exp(-\alpha z)-\frac{\alpha}{\beta_1}\times\frac{\cosh[\beta_1(z-L)]-\exp(-\alpha L)\cosh(\beta_1 z)}{\sinh(\beta_1 L)}\right)d\delta, \tag{4}$$

where $T(r,z,s)$ and $F(s)$ are, respectively, the time Laplace transform of the sample rise temperature and of the temporal form factor, $\beta_1=\sqrt{\delta^2+(s/D_1)}$, and δ is the spatial frequency. It should be noted that Eq. (4) is applicable if the heat diffusion in air is neglected. This happens when the ratio between the thermal effusivities of sample and air is larger than one [$e_1/e_0\gg 1$, where $e_i=k_i/\sqrt{D_i}=\sqrt{k_i(\rho c)_i}$]. This condition is usually verified for many solid samples due to the low value of k_0 and $(\rho c)_0$.

Therefore, by using Eqs. (1) and (4) and neglecting the deflection in air [the efficient path in Eq. (1) is from $z=0$ to $z=L$], one obtains the time Laplace transform of the deflection angle,

$$\Phi(r,s)=-\frac{1}{n}\frac{\partial n}{\partial T}F(s)\frac{\tau E[1-\exp(-\alpha L)]}{2\pi k_1}\times\int_0^\infty\frac{\delta^2 J_1(\delta r)\exp[-(\delta a)^2/8]}{\delta^2+\frac{s}{D_1}}d\delta. \tag{5}$$

By the use of the inverse Laplace transform and integrating over δ, the deflection angle for a pulse in the form of a Dirac delta function is given by

$$\Phi(r,t)=-\frac{1}{n}\frac{\partial n}{\partial T}\frac{8\tau E D_1[1-\exp(-\alpha L)]}{\pi k_1}\times\frac{r\exp[-2r^2/(a^2+8D_1t)]}{(a^2+8D_1t)^2}, \tag{6}$$

where D_1 is the sample thermal diffusivity, r is the distance between the two beam axes, and k_1 is the sample thermal conductivity.

Studying Eq. (6) one sees that the form of $\Phi(r,t)$ has two maxima as a function of r located symmetrically with respect to $r=0$, for which $\partial\Phi(r,t)/\partial r=0$, at positions

$$r_{\max}=\pm\frac{\sqrt{a^2+8D_1t}}{2}. \tag{7}$$

On the other hand, studying the time behavior of $\Phi(r,t)$ [Eq. (6)] one can see that the deflection angle reaches a maximum value at $t=0$, if $r<a$, while for $r>a$, it has a maximum at a later time $t_{\max}$ given by

$$t_{\max}=\frac{r^2-a^2}{8D_1}. \tag{8}$$

This behavior shows that the delay with which $\Phi(r,t)$ reaches its maximum value, with respect to the time ($t=0$) at which the pump pulse is applied, exists starting from a minimum distance $r_{\min}=a$ between the probe and pump beam. For smaller values of r, the deflection has its maximum at $t=0$.

Equation (6) has been derived for an ideal probe beam of zero size (single ray). Taking into account the probe beam spot size b one obtains the expression (see Appendix A)

$$\Phi(r,t)=-\frac{1}{n}\frac{\partial n}{\partial T}\frac{8\tau E D_1[1-\exp(-\alpha L)]}{\pi k_1}\times\frac{r\exp[-2r^2/(a^2+b^2+8D_1t)]}{(a^2+b^2+8D_1t)^2}. \tag{9}$$

Equation (9) shows that the deflection is given by an effective spot size

$$a_{\text{eff}}^2=a^2+b^2. \tag{10}$$

Finally, for a pump beam with a pulse of finite time duration t_0 and rectangular shape, by using Eq. (5) one obtains

$$\Phi\equiv\begin{cases}-\frac{1}{n}\frac{\partial n}{\partial T}\frac{\tau E[1-\exp(-\alpha L)]}{2\pi k_1 t_0}\frac{\exp[-2r^2/(a_{\text{eff}}^2+8D_1t)]-\exp(-2r^2/a_{\text{eff}}^2)}{r}, & 0<t<t_0,\\ -\frac{1}{n}\frac{\partial n}{\partial T}\frac{\tau E[1-\exp(-\alpha L)]}{2\pi k_1 t_0}\frac{\exp[-2r^2/(a_{\text{eff}}^2+8D_1t)]-\exp\{-2r^2/[a_{\text{eff}}^2+8D_1(t-t_0)]\}}{r} & t>t_0.\end{cases} \tag{11}$$

From the previous results one sees that at a distance $r>a_{\text{eff}}$ from the pump beam axis it is possible to have a deflection signal which reaches its maximum value at some time $t_{\max}$. In the case in which $t_{\max}\gg t_0$ and for $r>a_{\text{eff}}$, Eqs. (11) and (9) give for the thermal diffusivity of sample practically the same result,

$$D_1=\frac{r^2-(a^2+b^2)}{8t_{\max}}. \tag{12}$$

In a typical experiment $t_{\max}$ and r can be measured, while a_{eff}^2 is not known exactly. If D_1 has to be determined through Eq. (12), a number of determinations of $t_{\max}$ is made as a function of r. A plot of $t_{\max}$ as a function of r^2 is a straight line whose slope is $8D_1$ while the intercept at $t_{\max}=0$ is $r^2=a_{\text{eff}}^2$. In this way both the diffusion constant and the effective spot size are determined.

In Fig. 2 are shown the results of the theoretical calculation of the deflection angle Φ, reported to its maximum

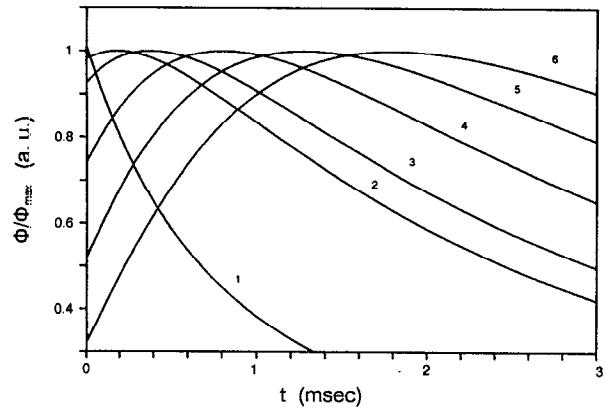

FIG. 2. Theoretical results of the deflection angle reported to its maximum value $\Phi(t)/\Phi_{max}$ vs the time delay t (ms) for different values of the pump-probe distance r ($D_1=0.005$ cm^2/s, $a_{eff}=70$ μm): (1) $r=35$ μm; (2) $r=75$ μm; (3) $r=80$ μm; (4) $r=90$ μm; (5) $r=100$ μm; (6) $r=110$ μm.

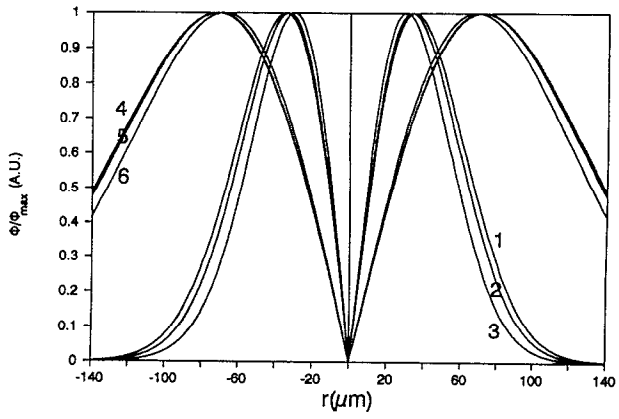

FIG. 4. Theoretical results of the deflection angle reported to its maximum value $\Phi(t)/\Phi_{max}$ vs the pump-probe offset r for different observation times and different pulse time lengths ($a_{eff}=40$ μm, $D_1=0.005$ cm^2/s): (1) $t=1$ ms, $t_0=1$ μs; (2) $t=1$ ms, $t_0=200$ μs; (3) $t=1$ ms, $t_0=500$ μs; (4) $t=5$ ms, $t_0=1$ μs; (5) $t=5$ ms, $t_0=200$ μs; (6) $t=5$ ms, $t_0=1000$ μs.

value, as a function of time for six different values of r, by the help of Eq. (9). It is evident that the maximum signal value position is very sensitive to the r value for $r>a_{eff}$. Figure 3 shows that a change of 20% of the thermal diffusivity value results in a corresponding change of the t_{max}; therefore, Eq. (9) is sensitive to any change of D_1. Figure 4 shows the theoretical results (see Eq. 11) of the deflection angle as a function of the distance between the centers of the two laser beams r for different observation times and different pulse time lengths. Note that the space maximum of deflection signal depends on the observation time, while it is insensitive enough to the pulse time length t_0. The different slope of the curves is due to the heat diffusion.

III. EXPERIMENTAL SETUP

The experimental setup is shown in Fig. 5. A beam from an Ar laser model Coherent Innova 70 has been used as a pump with an exit spot size of 0.75 mm, focused down to 42 μm from lens L_2 of focal length 0.2 m on an acousto-optic modulator from Hamamatsu. A diaphragm D is used to select the modulated beam that is sent on the sample through a moving mirror M, which is moved along the z direction so as to shift the pump beam on the sample with respect to the probe beam along the r direction. The probe beam comes from a He-Ne laser with a spot size at the exit of 0.4 mm. The probe is expanded four times by a beam expander BE and then is focalized by lens L_1 of focal length 0.1 m on the sample. The spot size on the sample is $b_0=22$ μm and the Rayleigh length is $z_b=0.24$ cm.

An interferential filter IF selects only the probe beam to be detected by the position sensor PS. The focal lengths of lenses L_2 and L_3 are chosen so to have a spot size on the sample $a_0=15$ μm, a value nearly equal to the spot size of the probe beam.

The pump Rayleigh length is, in this case, $z_a=0.145$ cm. The lens and the mirror M are mounted on a micrometric translator TLF8 Micro Control that allows one to perform a spatial scanning along the r axis.

The sample S is put on a similar translator which moves it along the z axis so as to change the spot sizes of both the pump and probe beams according to the relations

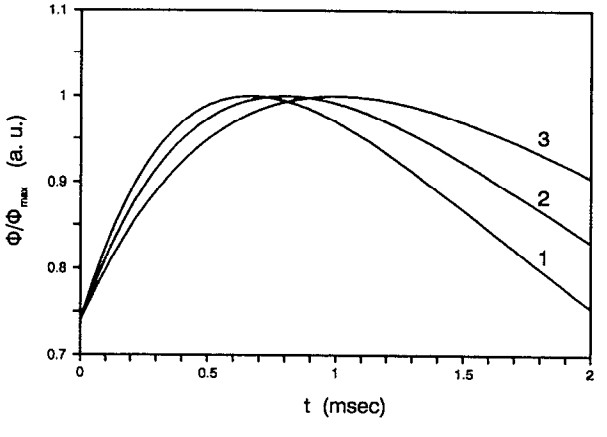

FIG. 3. Theoretical results of the deflection angle reported to its maximum value $\Phi(t)/\Phi_{max}$ vs the time delay t (ms) for different values of the sample diffusivity D_1 ($a_{eff}=70$ μm, $r=90$ μm): (1) $D_1=0.004$ cm^2/s; (2) $D_1=0.005$ cm^2/s; (3) $D_1=0.006$ cm^2/s.

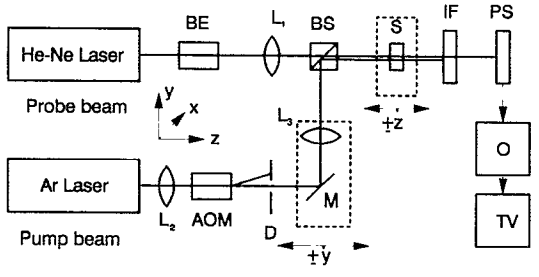

FIG. 5. Experimental setup.

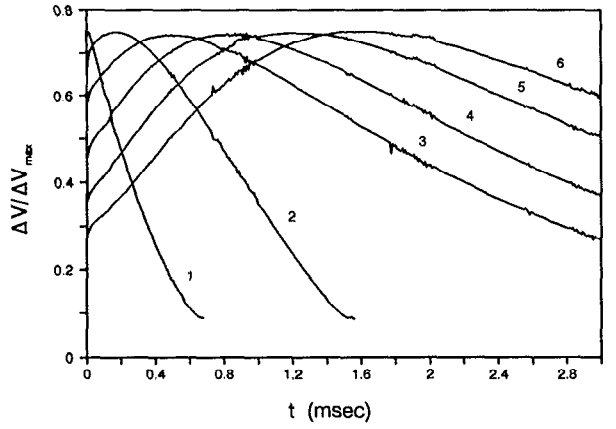

FIG. 6. Experimental results of the deflection signal reported to its maximum value $\delta V(t)/\Delta V_{max}$ vs time delay t (ms) for a glass doped with CdS-CdSe for different values of the pump-probe offset r (t_0=0.5 ms, P_{peak}=0.2 W): (1) r=30 μm; (2) r=70 μm; (3) r=80 μm; (4) r=90 μm; (5) r=100 μm; (6) r=110 μm.

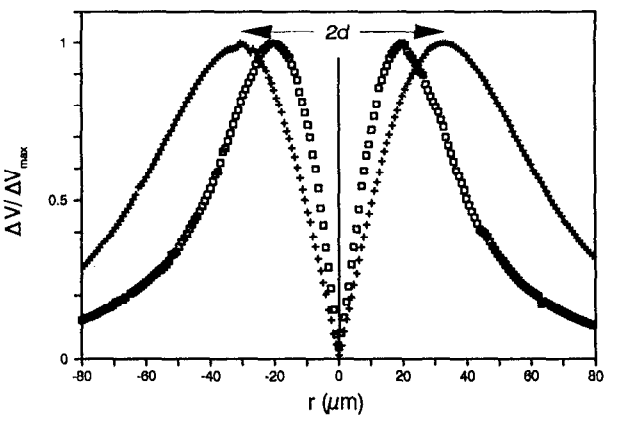

FIG. 7. Experimental results of the effective value of the deflection signal reported to its maximum value $\Delta V_{avg}(r)/\Delta V_{max}$ vs pump-probe offset r (μm) (t_0=0.2 ms, P_{peak}=0.2 W): (□) z=0.17 cm; (+) z=0.37 cm.

$$b(z)=b_0\sqrt{1+(z^2/z_b^2)},$$
$$a(z)=a_0\sqrt{1+(z^2/z_a^2)}. \tag{13}$$

A position sensor was used to detect the probe beam deflected by the sample heating. Its output is sent to an oscilloscope and a digital TV set.

Special care has been used to have the pump and probe beams in the same plane in which the deflection is produced by the heating of the sample; in our case the r-z plane.

IV. EXPERIMENTAL RESULTS

The method has been applied to measure the thermal diffusivity of a borosilicate glass doped with particles of CdS_xSe_{1-x}. The sample had 0.3 cm thickness. The probe beam was weakly absorbed (α=4 cm^{-1}) while the pump beam was strongly absorbed ($\alpha\approx 10^2$–10^3 cm^{-1} at 488 nm wavelength).

The optical penetration length of the pump beam is 10–100 μm, which is much shorter than the Rayleigh length (z_a=1450 μm) so we can consider the spot size inside the sample to have a fixed value even if the sample is not in the focus.

The peak power of the pulses of the Ar laser was P_{peak}=0.2 W, with a pulse time duration t_0=0.2–0.5 ms.

In Fig. 6 the deflection signal of the probe beam as a function of time is given for different distances r between the axis of the probe and pump beams (1-2-3-4-5-6). The starting point r=0 where pump and probe are superposed is easily found because it is the position in which the deflection signal goes to zero.

All curves have been normalized to their maximum value. The time t=0 on the plot corresponds to the time at which the pump pulse ends.

Curve 1 has been taken in the position $r=d$=30 μm at which a maximum value of the effective deflection signal occurs (see Fig. 7), while t_{max}=0 causes $d<a_{eff}$ [see Eq. (8)]. By increasing the distance r, the curves become wider and the value t_{max} shifts to longer times.

Figure 7 gives the effective value of the deflection signal measured with a lock-in amplifier as a function of r for two different values of the vertical offset z. The experimental results take into account a time average performed because of the integration time of the detection system (see Appendix B). By increasing z and accordingly a_{eff}, the distance $2d$ between the two maxima of the effective deflection signal increases due to the relation

$$d=\frac{a_{eff}}{2}\gamma\left(\frac{8D_1T_{avg}}{a_{eff}^2}\right), \tag{14}$$

where $\gamma(8D_1T_{avg}/a_{eff}^2)$ is the corrective function (see Appendix B) (plotted in Fig. 12) which always is greater than 1 ($1<\gamma<1.5852$), and T_{avg} is the time integrating constant of the detection system.

The values of time at which the deflection signal reaches its maximum value, t_{max}, as a function of r^2 for a pulse duration t_0=0.5 ms and for five different z values are shown in Fig. 8. By increasing z and accordingly a_{eff}, the slope does not change and the curves only shift parallel to each other in agreement with Eq. (12).

In Fig. 9 the behavior of t_{max} as a function of the pulse time length t_0 is shown for several values of r at fixed z (z=0.3 mm). By increasing t_0, t_{max} decreases according with Eq. (11).

V. DISCUSSION

From Eq. (12) we see that, when the center of the probe beam is at a suitable distance r from the center of the pump beam ($r>\sqrt{a^2+b^2}$), the time needed for the deflection signal to reach its maximum value t_{max} depends on the square of the distance r in a linear way,

$$r^2=c_1t_{max}+c_2, \tag{15}$$

where $c_1=8D_1$ and $c_2=a_{eff}^2=a^2+b^2$.

The curve $r^2=f(t_{max})$ is therefore a straight line with a slope proportional to the sample diffusivity, given by

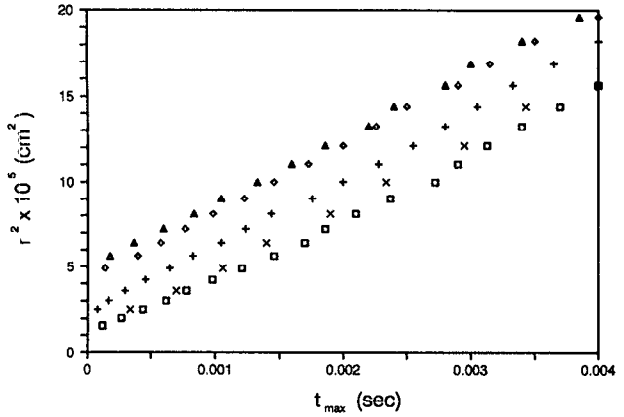

FIG. 8. Experimental results of the square pump-probe distance r^2 (cm^2) vs t_{max} (s) for different values of the vertical offset z (t_0=0.5 ms, P_{peak}=0.2 W): (□) z=0 cm; (×) z=0.03 cm; (+) z=0.17 cm; (♦) z=0.37 cm; (△) z=0.47 cm.

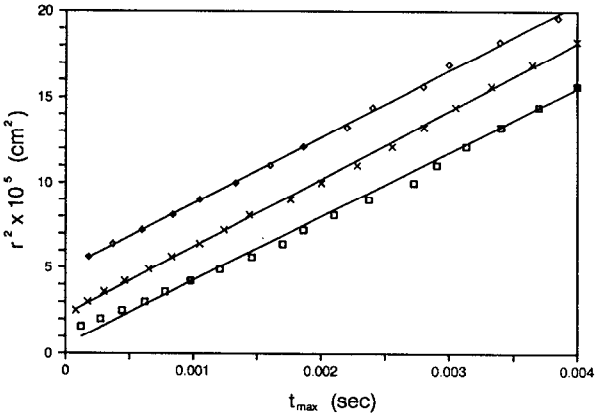

FIG. 10. Experimental behavior of the square of the pump-probe offset r^2 (cm^2) with respect to the delay time t_{max} (s) for different vertical offset z (t_0=0.5 ms, P_{peak}=0.2 W): (□) z=0 cm; (×) z=0.17 cm; (♦)=0.47 cm.

$$\frac{\Delta r^2}{\Delta t_{max}} = c_1 = 8D_1, \tag{16}$$

while the intercept with the r^2 axis, obtained for $t_{max}=0$, only depends on the effective spot size

$$r^2(t_{max}=0) = c_2 = a^2 + b^2 = a_{eff}^2. \tag{17}$$

Figures 10 and 11 show the experimental slopes for different values of z for two different pulse lengths: t_0=0.5 ms (Fig. 10) and t_0=0.2 ms (Fig. 11). Different values of z mean different positions of the sample along the z axis, i.e., different values of $a(z)$ and $b(z)$ [see Eq. (13)]. The continuous straight line is the result of a linear interpolation of Eq. (15) using the least-squares method. Note that by increasing z, i.e., $a^2(z)+b^2(z)$, the curves remain parallel to each other and only shift upward. Such behavior shows a good agreement between theory and experimental results.

In Table I are shown the values of D_1 and a_{eff} (columns 3 and 8), for different z values and for two different pulse lengths t_0 (columns 1 and 2), and the distance $2d$ between the two maxima of the effective deflection signal (column 4) obtained from the experimental data by using Eqs. (16) and (17). The calculated γ corrective function is reported in the column 5; the spot sizes of the two beams $a(z)$ and $b(z)$ calculated by the use of Eq. (13) are given in columns 6 and 7.

Finally, a comparison between the effective spot size $a_{eff}(z)$, obtained with different formulas [Eqs. (14) and (13)] (columns 9 and 10) and the value obtained by the experiments (column 8), is given showing a very good agreement.

An excellent agreement is also found between the values of thermal diffusivity measured with this method (column 3) and the ones obtained with the traditional photo-

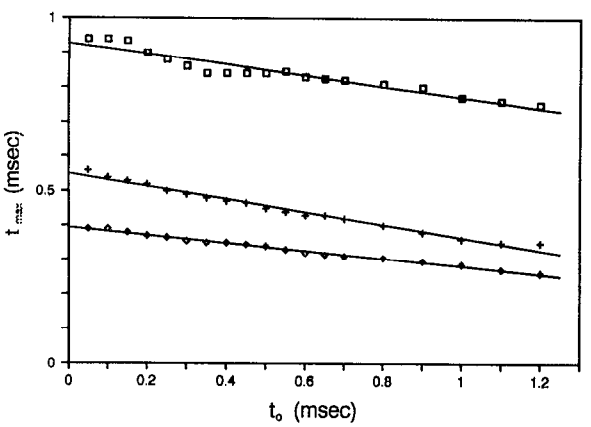

FIG. 9. Experimental behavior of the delay time t_{max} (ms) with respect to the pulse time length t_0 (ms) for different values of the pump-probe offset r (P_{peak}=0.2 W): (□) r=80 μm; (+) r=65 μm; (♦) r=60 μm.

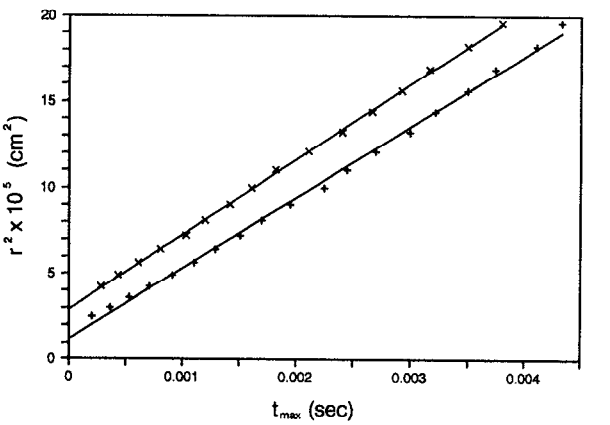

FIG. 11. Experimental behavior of the square of the pump-probe offset r^2 (cm^2) with respect to the delay time t_{max} (s) for different vertical offset z (t_0=0.2 ms, P_{peak}=0.2 W): (continuous line) linear interpolation; (+) z=0.17 cm; (×) z=0.37 cm.

TABLE I. Experimental data: In each row seven different experiments are shown, in each column all calculated parameters are reported. 1: time pulse length t_0 (ms); 2: vertical offset z (cm); 3: sample diffusivity D_1 (cm^2/s) obtained as $c_1/8$, 4: the distance $2d$ (μm) between the two maxima of the effective deflection signal; 5: the calculated γ corrective function; 6: pump beam spot size [Eq. (13)] 7: probe beam spot size [Eq. (13)]; 8: estimate of the effective spot size a_{eff} (μm) through Eq. (17); 9: estimate of the effective spot size a_{eff} (μm) through Eq. (14); 10: estimate of the effective spot size a_{eff} (μm) through Eq. (13).

1	2	3	4	5	6	7	8	9	10
t_0 (ms)	z (cm)	$D_1=\frac{c_1}{8}$	$2d$ (μm)	γ	$a(z)$ (μm) Eq. (13)	$b(z)$ (μm) Eq. (13)	$a_{eff}(z)$ (μm) Eq. (17)	a_{eff} (μm) Eq. (14)	$a_{eff}(z)$ (μm) Eq. (13)
0.2	0.17	0.0051	40	1.19	23	27	35	33.5	36
0.2	0.37	0.0053	60	1.106	41	40	54	54	58
0.5	0	0.0047	38	1.42	15	22	23	26.5	26
0.5	0.03	0.0050	40	1.38	15.5	22	27	29	27
0.5	0.17	0.0050	52	1.26	23	27	47	41.5	36
0.5	0.37	0.0049	64	1.15	41	40	66	55.5	58
0.5	0.47	0.0049	74	1.14	51	48	70	65	70

thermal deflection.[7–9] Note that this value is nearly insensitive to a bad focalization of the two beams on the sample.

VI. CONCLUSIONS

We have applied the photothermal deflection method in a modified collinear configuration with a pulsed pump beam to measure the thermal diffusivity of a transparent sample (with respect to the probe beam). In this method the time at which the maximum deflection of the probe beam traveling at a suitable distance from the pump is detected. We have taken into account the finite dimension of the probe beam and studied the effect of a nonperfect focalization of the beams on the sample. A very easy and accurate measurement of the thermal diffusivity can be performed in this way.

APPENDIX A

Starting from the relationship for the deflection angle of a single ray Φ_{ray} one may calculate the deflection angle of a beam Φ_{beam} by adding the individual deflections of each ray weighted over the beam intensity profile. Assuming a Gaussian profile with a spot size b, one can write[10]

$$\Phi_{beam}(x,y,t)=\frac{\int\int_{-\infty}^{+\infty}\Phi_{ray}(\xi,\eta,t)\exp\{-2[(x-\xi)^2+(y-\eta)^2]/b^2\}d\xi\,d\eta}{\int\int_{-\infty}^{+\infty}\exp\{-2[(x-\xi)^2+(y-\eta)^2]/b^2\}d\xi\,d\eta},$$

where $C\equiv(x,y)$ is the probe beam center and $\Gamma\equiv(\xi,\eta)$ is the position of the single ray. By using the polar coordinates

$$r=\sqrt{x^2+y^2},\quad \varphi=\arctan\frac{y}{x},$$

$$\rho=\sqrt{\xi^2+\eta^2},\quad \varphi_0=\arctan\frac{\eta}{\xi},$$

one determines that the deflection occurs along the r direction between the centers of the two beams, with intensity given by

$$\Phi_{beam}(r,t)=\frac{2}{\pi b^2}\int_{-\infty}^{+\infty}\Phi_{ray}(\rho,t)\rho\exp\left(-2\frac{\rho^2+r^2}{b^2}\right)d\rho\int_0^{2\pi}\exp\left(\frac{4\rho r}{b^2}\cos(\varphi-\varphi_0)\right)\cos(\varphi-\varphi_0)d\varphi_0$$

$$=\frac{4}{b^2}\exp\left(-2\frac{r^2}{b^2}\right)\int_0^{+\infty}\Phi_{ray}(\rho,t)\rho\exp\left(-2\frac{\rho^2}{b^2}\right)I_1\left(\frac{4\rho r}{b^2}\right)d\rho,$$

which, by the use of Eq. (6), becomes

$$\Phi_{beam}(r,t)=-\frac{1}{n}\frac{\partial n}{\partial T}\frac{8\tau E D_1[1-\exp(-\alpha L)]}{\pi k_1}\frac{4\int_0^{+\infty}\rho^2\exp\{-2[\rho^2(a^2+b^2+8D_1t)/b^2(a^2+8D_1t)]\}I_1\left(\frac{4\rho r}{b^2}\right)d\rho}{b^2(a^2+8D_1t)^2},$$

which under integration[11] gives

$$\Phi_{\text{beam}}(r,t)=-\frac{1}{n}\frac{\partial n}{\partial T}\frac{8\tau E D_1[1-\exp(-\alpha L)]}{\pi k_1}\times\frac{r\exp\{-2[r^2/(a^2+b^2+8D_1t)]\}}{(a^2+b^2+8D_1t)^2}$$

$$=\Phi_{\text{ray}}(r,t)\,|_{\bar{a}^2=a^2+b^2}.$$

Therefore, the beam deflection is equal to the deflection of the single ray traveling through the center of the probe beam when the pump spot size is $\bar{a}=\sqrt{a^2+b^2}$.

APPENDIX B

The relationship between the deflection angle $\Phi(r,t)$ and the effective deflection angle $\Phi_{\text{avg}}(r)$ at the output of a lock-in time integrating system is given by

$$\Phi_{\text{avg}}(r)=\frac{1}{T_{\text{avg}}}\int_0^{T_{\text{avg}}}\Phi(r,t)dt,$$

where T_{avg} is the time integration constant. By using Eq. (9), one obtains

$$\Phi_{\text{avg}}(r)=-\frac{1}{n}\frac{\partial n}{\partial T}\frac{8\tau E D_1[1-\exp(-\alpha L)]}{\pi k_1}\frac{r}{T_{\text{avg}}}\times\int_0^{T_{\text{avg}}}\frac{\exp\left(\frac{-2r^2}{a_{\text{eff}}^2+8D_1t}\right)}{(a_{\text{eff}}^2+8D_1t)^2}dt$$

$$=-\frac{1}{n}\frac{\partial n}{\partial T}\frac{\tau E[1-\exp(-\alpha L)]}{2\pi k_1}\times\frac{\exp\left(\frac{-2r^2}{a_{\text{eff}}^2+8D_1T_{\text{avg}}}\right)-\exp\left(\frac{-2r^2}{a_{\text{eff}}^2}\right)}{rT_{\text{avg}}}.$$

The effective deflection angle $\Phi_{\text{avg}}(r)$ has its maximum value for $r_{\max}=d$ (see Fig. 7), which could be calculated by the solution of $\partial\Phi_{\text{avg}}(r)/\partial r=0$ giving the relation

$$d=\frac{a_{\text{eff}}}{2}\gamma(\chi)\quad\text{with}\quad 1<\gamma(\chi)<1.585,$$

where $\gamma(\chi)$ is a corrective function taking into account the heat diffusion, given by

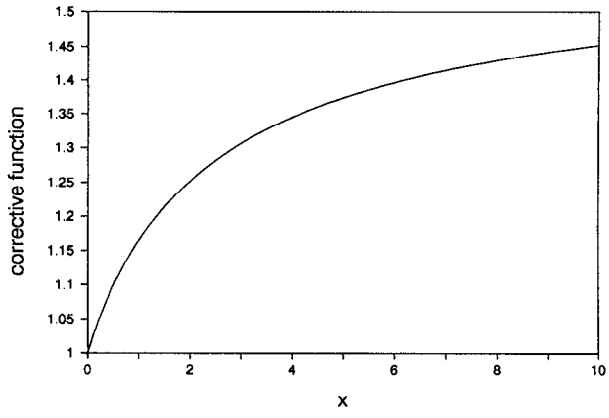

FIG. 12. The representation of the corrective γ function vs its argument $\chi=8D_1T_{\text{avg}}/a_{\text{eff}}^2$.

$$\frac{(\chi+1)(\gamma^2+1)}{\gamma^2+\chi+1}=\exp\left(\frac{\gamma^2\chi}{2(\chi+1)}\right),$$

where $\chi=8D_1T_{\text{avg}}/a_{\text{eff}}^2$. Figure 12 shows the plot of the function $\gamma(\chi)$. A numerical calculation put into evidence that $\gamma(\chi)$ has an increasing monotonic behavior and its values are in the range 1–1.585.

ACKNOWLEDGMENTS

Work performed under PF Materiel Specieli CNR with partial support from GNEqP of CNR and INFM.

[1] W. B. Jackson, N. M. Amer, A. C. Boccara, and D. Fournier, Appl. Opt. **20**, 1333 (1981).
[2] A. Rose, R. Vyas, and R. Gupta, Appl. Opt. **24**, 4626 (1986).
[3] A. C. Tam, in *Photothermal Investigation of Solids and Fluids*, edited by J. A. Sell (Academic, New York, 1988), Chap. 1.
[4] M. Bertolotti, L. Fabbri, E. Fazio, R. Li Voti, G. Liakhou, and C. Sibilia, J. Appl. Phys. **69**, 3421 (1991).
[5] W. J. Parker, R. J. Jenkins, C. P. Butler, and G. L. Abbott, J. Appl. Phys. **32**, 9 (1961).
[6] L. Fabbri and E. Scafè, Rev. Sci. Instrum. **63**, 2008 (1992).
[7] M. A. Shannon, A. A. Rostani, and R. E. Russo, J. Appl. Phys. **71**, 53 (1992).
[8] M. Bertolotti, R. Li Voti, G. Leakhou, and C. Sibilia, Rev. Sci. Instrum. **69**, 1576 (1993).
[9] M. Bertolotti, A. Ferrari, C. Sibilia, G. Suber, D. Apostol, and P. Jani, Appl. Opt. **27**, 1811 (1988).
[10] E. Legal Lasalle, F. Lepoutre, and J. P. Roger, J. Appl. Phys. **64**, 1 (1988).
[11] I. S. Gradshteyn and I. M. Ryzhik, *Table of Integrals Series and Products* (Academic, New York, 1980), p. 717.